University of Birmingham

University of Birmingham Research at Birmingham

Identification of Phosphorylation Sites Altering Pollen Soluble Inorganic Pyrophosphatase Activity

Eaves, Deborah J; Haque, Tamanna; Tudor, Richard L; Barron, Yoshimi; Zampronio, Cleidiane G; Cotton, Nicholas P J; de Graaf, Barend H J; White, Scott A; Cooper, Helen; Franklin, F Christopher H; Harper, Jeffrey F; Franklin-Tong, Vernonica E

[Link to publication on Research at Birmingham portal]

Identification of Phosphorylation Sites Altering Pollen Soluble Inorganic Pyrophosphatase Activity[1][CC-BY]

Deborah J. Eaves[2], Tamanna Haque[2,3], Richard L. Tudor[4], Yoshimi Barron[5], Cleidiane G. Zampronio[6], Nicholas P. J. Cotton, Barend H. J. de Graaf[7], Scott A. White, Helen J. Cooper, F. Christopher H. Franklin, Jeffery F. Harper, and Vernonica E. Franklin-Tong*

School of Biosciences, College of Life and Environmental Sciences, University of Birmingham, B15 2TT Birmingham, United Kingdom (D.J.E., T.H., R.L.T., C.G.Z., N.P.J.C., B.H.J.d.e.G., S.A.W., H.J.C., F.C.H.F., V.E.F.-T.); and Department of Biochemistry and Molecular Biology, University of Nevada, Reno, Nevada 89557 (Y.B., J.F.H.)

ORCID IDs: 0000-0002-6122-3377 (D.J.E.); 0000-0002-3979-8721 (T.H.); 0000-0003-0934-0792 (C.G.Z.); 0000-0003-0542-5510 (B.H.J.d.G.); 0000-0002-0202-6154 (S.A.W.); 0000-0003-4590-9384 (H.J.C.); 0000-0003-3507-722X (F.C.H.F.); 0000-0003-1782-8413 (V.E.F.-T.).

Protein phosphorylation regulates numerous cellular processes. Identifying the substrates and protein kinases involved is vital to understand how these important posttranslational modifications modulate biological function in eukaryotic cells. Pyrophosphatases catalyze the hydrolysis of inorganic phosphate (PP_i) to inorganic phosphate P_i, driving biosynthetic reactions; they are essential for low cytosolic inorganic phosphate. It was suggested recently that posttranslational regulation of Family I soluble inorganic pyrophosphatases (sPPases) may affect their activity. We previously demonstrated that two pollen-expressed sPPases, Pr-p26.1a and Pr-p26.1b, from the flowering plant *Papaver rhoeas* were inhibited by phosphorylation. Despite the potential significance, there is a paucity of data on sPPase phosphorylation and regulation. Here, we used liquid chromatographic tandem mass spectrometry to map phosphorylation sites to the otherwise divergent amino-terminal extensions on these pollen sPPases. Despite the absence of reports in the literature on mapping phosphorylation sites on sPPases, a database survey of various proteomes identified a number of examples, suggesting that phosphorylation may be a more widely used mechanism to regulate these enzymes. Phosphomimetic mutants of Pr-p26.1a/b significantly and differentially reduced PPase activities by up to 2.5-fold at pH 6.8 and 52% in the presence of Ca^{2+} and hydrogen peroxide over unmodified proteins. This indicates that phosphoregulation of key sites can inhibit the catalytic responsiveness of these proteins in concert with key intracellular events. As sPPases are essential for many metabolic pathways in eukaryotic cells, our findings identify the phosphorylation of sPPases as a potential master regulatory mechanism that could be used to attenuate metabolism.

Numerous cellular processes are regulated by reversible protein phosphorylation (Humphrey et al., 2015), including metabolism, cell cycle progression, differentiation, biotic and abiotic stress tolerance, and apoptosis. Many metabolic enzymes are regulated by phosphorylation. Identifying the targets, phosphorylation sites, and protein kinases involved is vital to understanding how these important posttranslational modifications affect biological functions. In flowering plants, there are more than 1,000 protein kinases, of which 34 in Arabidopsis (*Arabidopsis thaliana*) belong to a family of calcium dependent protein kinases (CPKs). CPK-related kinases have been implicated in regulating many aspects of plant biology, including pathogen defense, interactions with symbionts, abiotic stress responses, and pollen tube growth (Harper et al., 2004; Zulawski et al., 2014).

Pyrophosphatases (PPases) are ubiquitous, highly conserved phosphate-metabolizing enzymes that play a central role in cellular metabolism. Inorganic phosphate (PP_i) is produced within cells as a by-product of anabolic processes, such as nucleic acid and protein biosynthesis, as well as carbohydrate synthesis (including that of cell wall materials

required for pollen tube growth). Soluble inorganic pyrophosphatases (sPPases) catalyze the hydrolysis of inorganic pyrophosphate (PP_i) into two molecules of inorganic phosphate (P_i). The net release of energy from this reaction provides a thermodynamic driving force for many biosynthetic reactions, such as protein, polysaccharide, and nucleotide synthesis. PPases are the key enzymes that keep cytosolic [PP_i] low in cells. This is essential, as high [PP_i] is toxic (Cooperman et al., 1992). Removal of PPi is performed by two nonhomologous PPase enzymes. In animal cells and yeast, Family I sPPases are solely responsible (Pérez-Castiñeira et al., 2002; Serrano-Bueno et al., 2013), but in plants, the role of sPPases is disputed; it is hypothesized that their role has largely been taken over by the membrane-located proton-translocating PPases (Buchanan et al., 2002). Nevertheless, several examples have shown the importance of sPPases in metabolically active plant tissues; photosynthetic carbon assimilation and metabolism are greatly affected by changes in the levels of sPPases (Sonnewald, 1992; de Graaf et al., 2006; George et al., 2010). The structure and catalytic mechanisms of Family I sPPases are well characterized in

bacteria and the budding yeast *Saccharomyces cerevisiae* (Cooperman et al., 1992).

Given their biochemical function, not surprisingly, the activity of sPPases is essential for cellular metabolism and growth. Knockout of sPPase results in the arrest of cell division in *Escherichia coli* and inviability in budding yeast (Chen et al., 1990; Ogasawara, 2000; Pérez-Castiñeira et al., 2002), underlining the critical importance of PPi regulation. However, despite the cellular importance of [PP_i] homeostasis, mechanisms regulating Family I sPPase activity have not been studied thoroughly, especially in eukaryotic cells. It was generally accepted until recently that a reduction in sPPase activity causes the accumulation of PP_i to toxic levels, causing cell death. In bacteria, it has been suggested that posttranslational regulation of catalytic activity may play an important role in regulating the activity of sPPases (Kukko-Kalske et al., 1989). However, evidence for this is scarce. Although two studies have reported the phosphorylation of sPPases in vitro (Vener et al., 1990; Rajagopal et al., 2003), the sPPases from the flowering plant *Papaver rhoeas* (de Graaf et al., 2006) appear to be the only example with in vivo evidence for the phosphorylation of Family I eukaryotic sPPases modifying activity.

Cellular responses require an integrated signal perception and signal transduction network. During pollination, higher plants use specific interactions between male (pollen) and female (pistil) tissues. Many flowering plants utilize genetically controlled self-rejection systems: self-incompatibility (SI), to prevent self-fertilization and inbreeding. *P. rhoeas* uses an SI system involving the female *S*-determinant (PrsS) protein, which is a ligand secreted by the pistil (Foote et al., 1994), and the male *S*-determinant protein, PrpS (Wheeler et al., 2009). In this SI system, the interaction of pollen with self (incompatible) PrsS protein induces an influx of Ca^{2+} and K^+ (Wu et al., 2011) and transient increases in cytosolic free Ca^{2+} concentrations ([Ca^{2+}]$_{cyt}$) in incompatible pollen (Franklin-Tong et al., 1997). Downstream, SI triggers transient increases in reactive oxygen species (ROS) and nitric oxide, which participate in signaling alterations to the actin cytoskeleton and programmed cell death (PCD; Wilkins et al., 2011, 2014). SI also triggers dramatic acidification of the cytosol, which is necessary and sufficient to trigger PCD, involving the activation of a DEVDase/caspase-3-like activity (Bosch and Franklin-Tong, 2007; Wilkins et al., 2015). However, one of the earliest targets of the SI-mediated Ca^{2+} signals are a pair of pollen-expressed Family I sPPases, Pr-p26.1a and Pr-p26.1b (hereafter called p26a and p26b), that are rapidly phosphorylated in a Ca^{2+}-dependent manner in incompatible pollen after SI (Rudd et al., 1996). Increases in [Ca^{2+}]$_{cyt}$ and phosphorylation of these sPPases resulted in a reduction in their activity (de Graaf et al., 2006).

Here, we have mapped phosphorylation sites on p26a/b catalyzed by endogenous pollen kinases and recombinant CPKs. Using recombinant phosphomimetic p26a/b proteins, we provide evidence that the phosphorylation status of these sites is an important factor that differentially modulates the catalytic responsiveness of the two proteins in relation to key intracellular events that are triggered during the inhibition of pollen tube growth by SI. As the activity of PPases is crucial for all living eukaryotic cells, our findings provide an important conceptual advance in our general knowledge about the modulation of a major group of these essential housekeeping enzymes.

[2] These authors contributed equally to the article.

[3] Present address: Department of Horticulture, Bangladesh Agricultural University, Mymensingh 2202, Bangladesh.

[4] Present address: Elsoms Seeds, Spalding PE11 1QG, Lincolnshire, UK.

[5] Present address: Syngenta Crop Protection, Greensboro, NC 27409.

[6] Present address: School of Life Sciences, University of Warwick, Coventry CV4 7AL, UK.

[7] Present address: School of Biosciences, Cardiff University, Cardiff CF10 3XQ, UK.

* Address correspondence to v.e.franklin-tong@bham.ac.uk.

The author responsible for distribution of materials integral to the findings presented in this article in accordance with the policy described in the Instructions for Authors (www.plantphysiol.org) is: Vernonica E. Franklin-Tong (v.e.franklin-tong@bham.ac.uk).

V.E.F.-T., J.F.H., S.A.W., and F.C.H.F. conceived, designed, and supervised the experiments; D.J.E., T.H., Y.B., R.L.T., B.H.J.d.G., and C.G.Z. performed the experiments; N.P.J.C. provided technical assistance; H.J.C. contributed new reagents/analytic tools; D.J.E., T.H., N.P.J.C., and C.G.Z. analyzed the data; D.J.E. and S.A.W. prepared the final figures; V.E.F.-T. wrote the article with major contributions from J.F.H. and F.C.H.F.

RESULTS

p26a/b Have Activities Characteristic of Family I sPPases

The two *P. rhoeas* p26 sPPase sequences are highly conserved, with 79.5% amino acid identity between their core enzymatic regions. However, major variation occurs in their N-terminal regions (31.6% identity between 36 and 57 amino acid residues in p26a and p26b, respectively; Supplemental Fig. S1). The substrate specificities for recombinant p26a and p26b are

virtually identical, with preference for pyrophosphate (Supplemental Fig. S2; Supplemental Table S1). Both p26a and p26b have classic Mg^{2+}-dependent sPPase activities, with identical requirements for Mg^{2+} (not significant [NS], $P = 0.994$; Supplemental Fig. S2, Ai). Although divalent cations affect prokaryotic sPPase activities, there was no significant difference between p26a and p26b PPase activities at any concentrations tested for $ZnCl_2$ (NS, $P = 0.890$), Co^{2+} (NS, $P = 0.809$), or Mn^{2+} (NS, $P = 0.573$; Supplemental Fig. S2, Aii–Aiv). Ca^{2+} is a competitive inhibitor to Family I sPPases (Cooperman et al., 1992), and increasing $[CaCl_2]$ resulted in a loss of Mg^{2+}-dependent pyrophosphatase activity (50% inhibition of initial activity < 100 μM; Supplemental Fig. S2, Bi). The p26a/b PPase activities were strongly inhibited by F^- (like other eukaryotic Family I sPPases), but there was no differential response (NS, $P = 0.238$; Supplemental Fig. S2, Bii). As a large influx of K^+ is triggered by SI in incompatible pollen (Wu et al., 2011), we examined if K^+ affected the p26 PPase activities. K^+ did not inhibit their PPase activities, and they both behaved similarly in the presence of K^+ (NS, $P = 0.172$; Supplemental Fig. S2, Biii). Thus, p26a and p26b, without any phosphomodifications, exhibited virtually identical sPPase activities under various biologically relevant conditions.

In Vitro Phosphorylation of p26 Using Pollen Extracts

We previously demonstrated the Ca^{2+}-dependent phosphorylation of pollen-expressed sPPases, p26a and p26b, in living pollen tubes undergoing the SI response and a corresponding decrease in their PPases activity (Rudd et al., 1996; de Graaf et al., 2006). Here, we determined the sites phosphorylated on the His-tagged recombinant p26a/b proteins to gain insights into the functional significance of the phosphorylation. We performed liquid chromatographic tandem mass spectrometry (LC-MS/MS) using electron transfer dissociation (ETD) to map amino acid residues modified on p26a and p26b after phosphorylation by native *P. rhoeas* pollen kinases in pollen extracts. This analysis identified phosphorylation on Ser-13, Thr-18, and Ser-27 for p26a and phosphorylation on Thr-25, Ser-41, and Ser-51 for p26b (Fig. 1; Supplemental Fig. S1; Supplemental Table S2, A and B). Notably, all of the detectable phosphorylation sites were located in the N-terminal extensions.

Identification of CPKs That Can Phosphorylate p26 sPPases

As we showed previously that p26a/b were phosphorylated by a Ca^{2+}-dependent protein kinase (CPK)-type
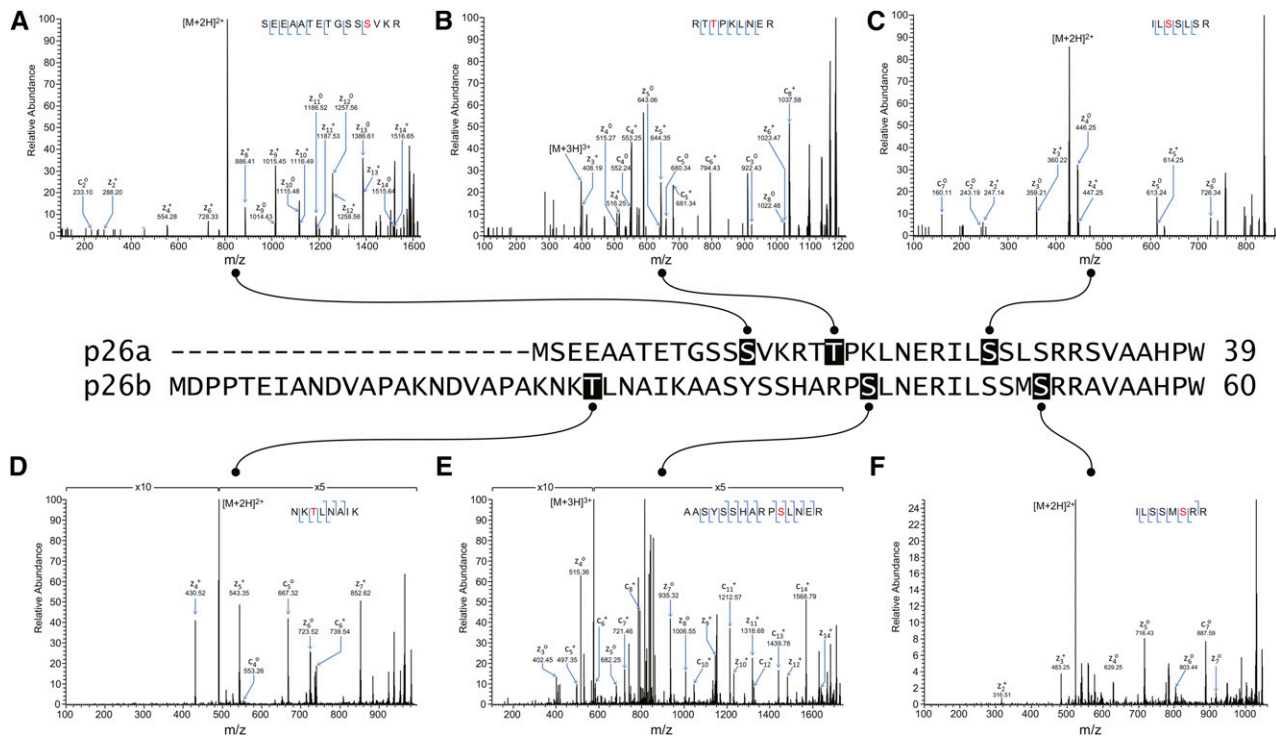
Figure 1. Phosphorylation sites identified by LC-MS/MS in recombinant p26 phosphorylated in vitro by endogenous pollen kinases. The sequence alignment of the N-terminal regions of the p26 sPPase proteins is annotated to indicate amino acid residues identified as phosphorylated by endogenous pollen kinases by LC-MS/MS. A to F show ETD mass spectra detected from p26a (A–C) and p26b (D–F) after phosphorylation using pollen extracts. A, Ser-13 phosphorylation recorded on +2 ions at mass-to-charge ratio (*m/z*) 809.85. B, Thr-18 phosphorylation recorded on +3 ions at *m/z* 399.19. C, Ser-27 phosphorylation detected on +2 ions at *m/z* 428.22. D, Thr-25 phosphorylation detected on +2 ions at *m/z* 491.25. E, Ser-41 phosphorylation detected on +3 ions at *m/z* 575.92. F, Ser-51 phosphorylation detected on +2 ions at *m/z* 523.24. S/T, Phosphorylated residues.

activity (Rudd et al., 1996), we tested to see if p26a/b was a substrate for AtCPK34, a CPK that is highly expressed in Arabidopsis pollen and required for pollen fitness (Harper et al., 2004; Myers et al., 2009). Using in vitro kinase assays, AtCPK34 phosphorylated p26a and p26b at levels severalfold greater than casein kinase II (CKII) and protein kinase A (PKA; Fig. 2, A and B). This confirms p26 as a potential target for CPK-mediated phosphorylation. Therefore, we initiated the cloning of *P. rhoeas* pollen-expressed orthologs and obtained cDNA clones for three *P. rhoeas* CPKs, *PrCPK14*, *PrCPK6/26*, and *PrCPK17/34*, named after their homology to three distinct groups of CPKs from Arabidopsis (Supplemental Fig. S3, A and B). These CPKs were engineered as recombinant His-tagged versions and used with in vitro kinase assays to assess whether the p26 proteins were substrates.

p26a/b Are Substrates of *P. rhoeas* Pollen-Expressed CPKs

All three His-tagged versions of the PrCPKs were able to phosphorylate syntide-2 (Supplemental Table
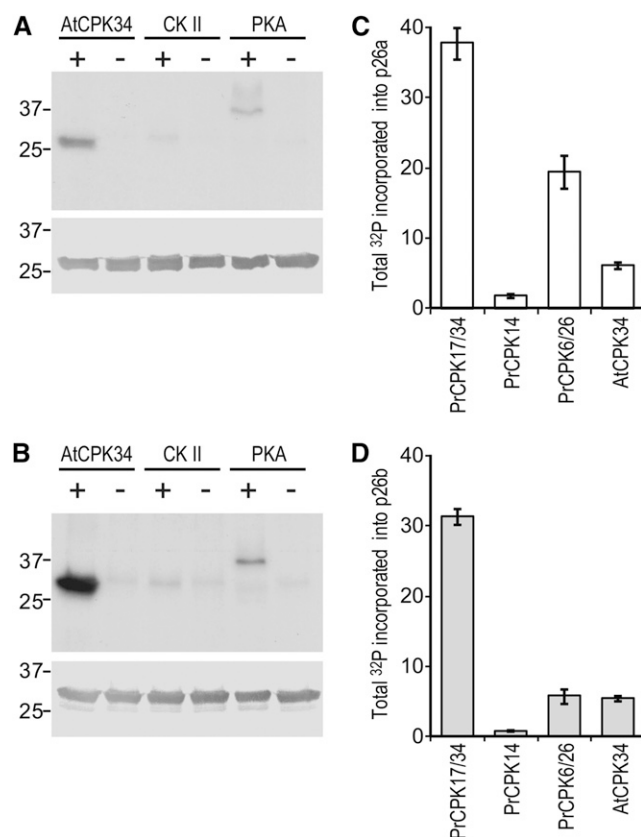
Figure 2. Phosphorylation of recombinant p26 by CPKs in vitro. A and B, Incorporation of ^{32}P into p26 after in vitro kinase assays using recombinant AtCPK34, CKII, or PKA with recombinant p26a (A) and p26b (B). Top gels are autoradiographs showing ^{32}P incorporation (total pmol), and bottom gels are western blots to show equal loading of protein. C and D, Incorporation of ^{32}P into p26a (C) and p26b (D) during in vitro phosphorylation using PrCPK17/34, PrCPK14, PrCPK6/26, or AtCPK34. Values are means ± SE ($n = 3$).

S3A) and p26a/b proteins (Fig. 2, C and D). Under Michaelis-Menten conditions, all three *P. rhoeas* CPKs had comparable K_m values for p26a/b, although the reaction rates (k_{cat}) varied (Supplemental Table S3, B and C). An LC-MS/MS analysis was used to ascertain which residues were phosphorylated after in vitro kinase assays (Fig. 3; Supplemental Table S2A). The overall protein sequence coverage of p26a and p26b peptides was virtually complete, at 93.5% to 95.3% coverage. No single CPK phosphorylated all sites identified. For p26a, ETD mass spectra revealed phosphorylation on Ser-11, Ser-12, Ser-13, Thr-17, Ser-27, Ser-28, Ser-30, and Ser-33. PrCPK17/34 showed broadest specificity and recognized all but Ser-33. While Ser-33 was phosphorylated by PrCPK14, this kinase did not appear to recognize Ser-11, Thr-17, Ser-27, and Ser-28. While a location in the N-terminal extension was observed for all phosphorylation sites in both p26a and p26b, the specific sequences surrounding the sites were different (Fig. 3; Supplemental Table S2B). Several of the sPPase amino acids phosphorylated by these PrCPKs were identical to those phosphorylated by the endogenous pollen kinases (Ser-13, Thr-18, and Ser-27 in p26a and Thr-25, Ser-41, and Ser-51 in p26b). Notably, the phosphorylated sites that mapped on p26a and p26b using the various recombinant CPKs were different.

Phosphomimic Substitutions Exhibit Unchanged sPPase Activities under Standard Conditions

To attempt to ascertain whether the mapped phosphorylation sites in p26a/b had any biological significance, we examined whether phosphomimic substitutions of key amino acids had any effect on the p26a/b PPase activities. To determine whether phosphorylation of these amino acid residues could attenuate PPase activity, we constructed phosphomimic (Glu substitution) and corresponding phosphonull (Ala substitution) His-tagged mutant p26a/b proteins (Supplemental Table S4, A and B). The triple substitution phosphomimic mutants for p26a [S13E, T18E, and S27E, named p26a(3E)] and p26b [T25E, S41E, and S51E, named p26b(3'E)] and their corresponding phosphonull versions comprised the sites phosphorylated by the endogenous pollen kinases. We measured their PPase activities and kinetic parameters for hydrolysis of PPi using recombinant p26 proteins. The K_m, turnover number (k_{cat}), and catalytic efficiencies of recombinant p26a and p26b were not significantly different ($P = 0.499$, $P = 0.991$, and $P = 0.448$ respectively; Supplemental Table S4, C and D). The kinetic parameters for PPi hydrolysis for the triple phosphomimic and phosphonull p26a and p26b mutants also were not significantly different from those for unmodified p26 sPPases (Supplemental Table S4, C and D), suggesting that phosphorylation of these residues alone is insufficient to alter the kinetics of these sPPases in vitro under these standard in vitro conditions. We constructed further phosphomutants with five and seven substituted residues mapped from in vitro phosphorylations with recombinant CPKs (Supplemental Table S4, A and B):
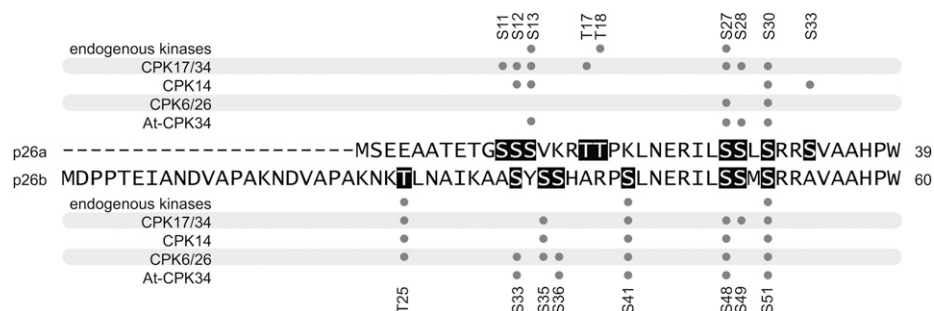
Figure 3. Phosphorylation sites identified by LC-MS/MS in p26 sPPase proteins phosphorylated by CPKs. The sequence alignment of the N-terminal regions of the p26 sPPase proteins is annotated to indicate phosphorylations by individual recombinant kinases and whole pollen extract. S/T, Phosphorylated residues.
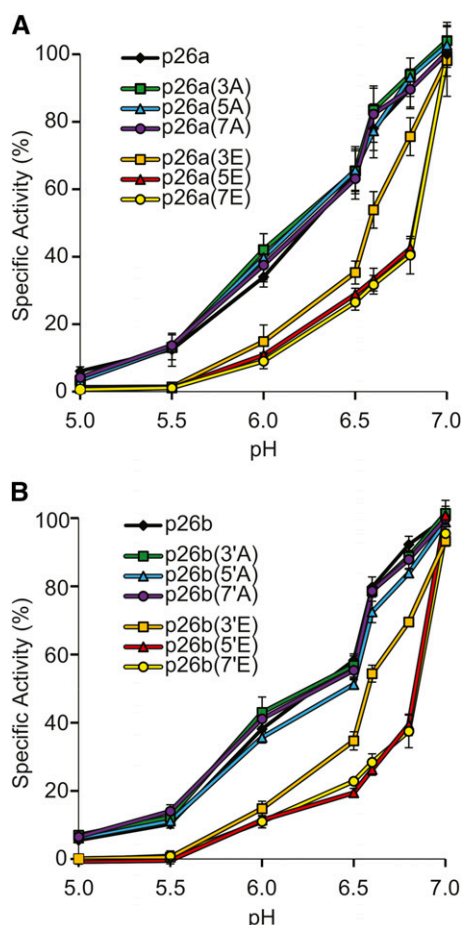

p26a(5E), p26b(5'E), p26a(7E), and p26b(7'E). There was no difference in activity between the wild-type p26a/b and phosphomimic/phosphonull mutants at pH 7 (Fig. 4; p26a [NS, $P = 0.772$] and p26b [NS, $P = 0.109$]).

pH Sensitivity Is Enhanced in p26 Phosphomimic Mutants

We previously demonstrated that SI triggers rapid, dramatic cytosolic acidification of incompatible pollen,

Figure 4. Effects of pH on PPase activities of p26a/b and their phosphonull and phosphomimic mutant versions. Recombinant p26 and mutant versions were assayed for PPase activity at variable pH. Values are means ± SE ($n = 4$). A, p26a. B, p26b.

with cytosolic pH ($[pH]_{cyt}$) decreasing from pH 7 to 6.8 within 10 min and to pH 5.5 within 60 min (Wilkins et al., 2015). Both p26a and p26b had identical pH profiles and displayed a pH-dependent attenuation typical of other Family I sPPases (Cooperman et al., 1992; Wilkins et al., 2015). Examining if pH affected the PPase activity of the phosphomimic mutants, we found that their activities were more sensitive to decreases in pH (Fig. 4). In contrast to activities at pH 7, at pH 6.8, a large drop in PPase activity of all the phosphomimic mutants was observed, significantly lower than in the wild type and the phosphonull mutants ($P = 0.000$; Fig. 4); the drop in activity of the 5E/5'E and 7E/7'E mutants was much larger than that of the 3E/3'E mutants (~42.5%–37.4% compared with 75.6%–69.5%; Fig. 4). The PPase activity of the phosphomimic mutants was completely inhibited below pH 5.5, significantly lower than wild-type and phosphonull mutant enzymes ($P = 0.002$ and $P = 0.000$, respectively), which retained residual activity at this pH. Thus, although these two pollen-expressed sPPases exhibited indistinguishable PPase activities under normal physiological (pH ~ 7) conditions and phosphomimic substitutions did not alter their kinetic parameters, at lowered pH, the phosphomimic mutants exhibited differential reductions in sPPase activity. This implicates phosphorylation as having an effect on p26 PPase activity when physiological pH drops and provides strong evidence that phosphorylation at several amino acid residues in the N-terminal region affects p26 PPase activity at low pH.

Ca²⁺ and Hydrogen Peroxide Additively Inhibit p26 Phosphomimic/Phosphonull Activities Differentially

The inhibitory effect of Ca^{2+} on PPases is well known (Cooperman et al., 1992); this is also the case for the *P. rhoeas* sPPases (Rudd et al., 1996; de Graaf et al., 2006). As SI triggers increases in $[Ca^{2+}]_{cyt}$ and phosphorylation of p26 in incompatible pollen preceding a ROS burst (Wilkins et al., 2011), we investigated the effect of hydrogen peroxide (H_2O_2) combined with Ca^{2+} on the recombinant p26 enzymes and their triple phosphorylation site substitution mutants at pH 7. This pH was chosen because the PPase activity of the wild-type enzyme is negligible at pH 5.5, making it difficult to quantify any additional negative contributions from

the phosphomimic mutants. Moreover, we thought that the physiologically most important question was to evaluate the enzymes under the conditions that would exist at the start of the SI response when the pH was ~7.

As expected, Ca^{2+} significantly inhibited the activity of all forms of p26 ($P = 0.000$). Notably, PPase activity in the phosphomimic mutants was more strongly inhibited by Ca^{2+} than their corresponding phosphonull mutants ($P = 0.000$; Fig. 5). Similarly, all the p26a phosphomimic mutants were significantly more sensitive to an H_2O_2 treatment ($P = 0.038$ for 3A versus 3E, $P = 0.030$ for 5A versus 5E, and $P = 0.022$ for 7A versus 7E; Fig. 5A), which also was the case for p26b (Fig. 5B). Combined Ca^{2+} and H_2O_2 had a much greater effect, with PPase activity less than 20% compared with untreated (Fig. 5). Thus, under these conditions, we established key phosphorylation sites that are important for modulating their activity. Maximal reduction in activity was achieved in the phosphomimic forms of p26a(3E)/b(3'E); additional phosphorylation site substitutions (5E and 7E) had no further effect. Thus, the triple phosphomimic forms of p26a/b (phosphorylation sites attributed to the endogenous pollen kinases) contributed to the enhanced inhibition by Ca^{2+} and H_2O_2.

Ca^{2+}, H_2O_2, and pH All Contribute to Inhibit p26 Activity

Having established that combining Ca^{2+} and H_2O_2 resulted in further reduced PPase activity prompted a related but subtly different question: if these conditions are combined with reduced pH (also triggered by SI but slightly later), does the sPPase activity decrease even further? Therefore, we measured the recombinant p26a/b sPPase activities with Ca^{2+} and H_2O_2 combined with several pH points relevant to SI. As shown earlier, we found that the PPase activities of both p26a and p26b were reduced significantly by Ca^{2+} and reduced further by Ca^{2+} combined with H_2O_2 (Fig. 6). As expected, the PPase activity for all of these observations was substantially reduced further by a reduction in pH,

and by pH 5.5, activity was ~10% (Fig. 6). The PPase activities of p26a treated with Ca^{2+}, H_2O_2, or Ca^{2+} and H_2O_2 were reduced and significantly different at each pH (Fig. 6A; $P = 0.005$, 0.003, 0.005, 0.017, and 0.014 by ANOVA at pH 7, 6.8, 6.5, 6, and 5.5, respectively). p26b behaved in a similar manner (Fig. 6B). At pH 5, the PPase activity for all the treatments was approximately zero, and none of the treatments were significantly different ($P = 0.660$ by ANOVA). These data demonstrate that all three SI-induced events can contribute to reduce sPPase activity.

Mapping of Phosphorylation Sites on CPKs

We also mapped several phosphorylation sites on recombinant forms of the three PrCPKs and AtCPK34 (Supplemental Table S5, A–C; Supplemental Data S1; Supplemental Fig. S4). This information is important for the plant CPK field. Notably, we mapped a phosphorylated Tyr (Tyr-82) on peptide VKSIYTIGKE in PrCPK17/34 that aligns to the same conserved Tyr residue within the kinase catalytic domain as identified in soybean (*Glycine max*) CPKβ (Tyr-24). This confirms the finding that CPKs can phosphorylate Tyr in plants (Oh et al., 2012) and is of interest, as very few Tyr phosphorylation sites have been identified for plant proteins and no bona fide Tyr kinases have been found (Sugiyama et al., 2008).

DISCUSSION

Identification of Phosphorylation Sites Identified on sPPases

It was suggested recently that posttranslational processes may play an important role in regulating the activity of Family I sPPases (Serrano-Bueno et al., 2013). However, studies reporting the phosphorylation of sPPases have been scarce. We previously identified the phosphorylation of two pollen-expressed Family I
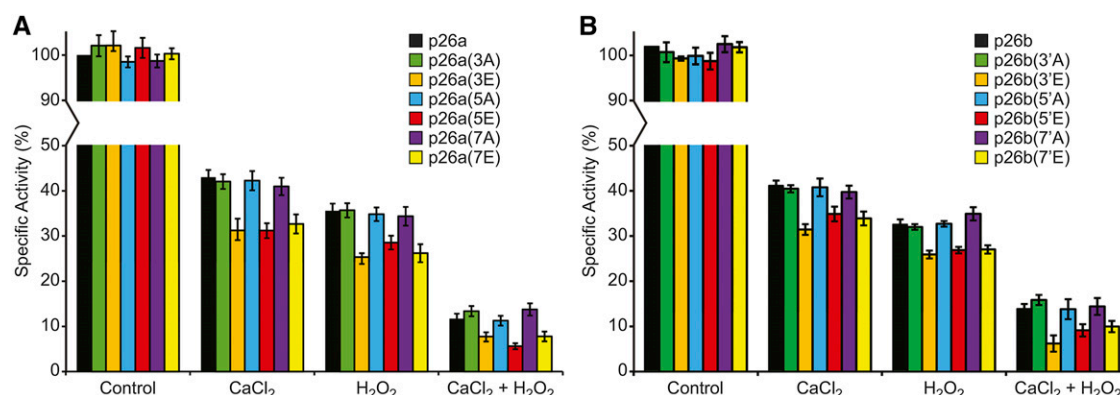
Figure 5. Ca^{2+} and H_2O_2 additively affect PPase activities of p26a/b and differentially affect their phosphonull and phosphomimic mutants. Recombinant p26 enzymes were assayed for PPase activity at pH 7 and supplemented with $CaCl_2$ and/or H_2O_2. Values are means $\pm$ SE ($n = 3$).
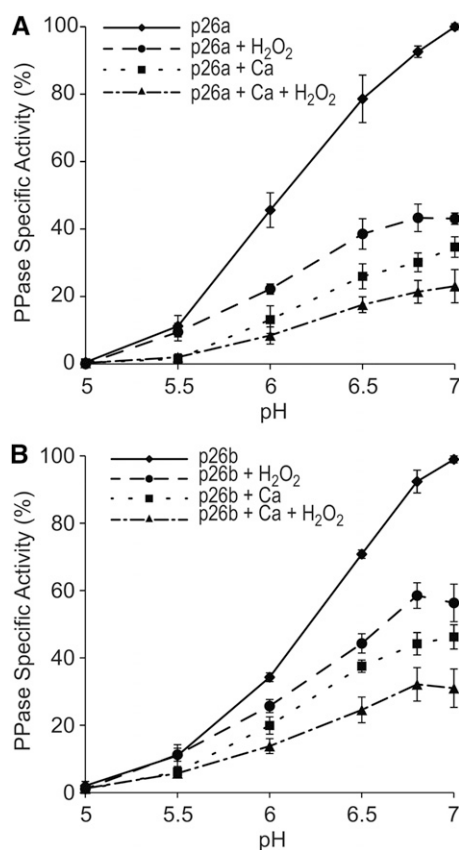
Figure 6. pH further reduces PPase activity in the presence of Ca^{2+} and H_2O_2. Recombinant sPPase p26a (A) and p26b (B) enzymes were assayed for PPase activity (diamonds) and in the presence of $CaCl_2$ (squares), H_2O_2 (circles), and $CaCl_2 + H_2O_2$ (triangles) at several pH levels. The activity for each was reduced further by lowered pH. Values are means ± SE ($n = 5$ for p26a and $n = 3$ for p26b).

identified at or near the catalytic active site, it is currently difficult to build a model of how the phosphorylation of eukaryotic sPPases might affect their enzymatic activity.

We also identified a Tyr residue that is phosphorylated in human PPA1 (Tyr-143) and mouse and *E. coli* sPPases. This site in *E. coli* (Tyr-142) has a role in binding to one of the two phosphates in the substrate. Our finding suggests that phosphorylation at this site may play a role in regulating PPase activity in some eukaryotes, as the active site and this Tyr are highly conserved across all family I PPases. The phospho-Tyr would both sterically clash and electrostatically repel PPi binding at the active site, affecting substrate binding and enzyme catalytic activity. The identification of phosphorylated amino acid residues in a number of species provides an important foundation for exploring the basis of these posttranslational modifications of these important enzymes and their biological consequences in the future. Whether there is an analogous phospho-Tyr modification during an SI response is uncertain. However, we did obtain evidence that the three PrCPKs and AtCPK34 tested here for in vitro activities are dual-specificity kinases (Oh et al., 2012; Supplemental Table S5, A–C; Supplemental Fig. S4), which leaves open their potential to function in planta as a Tyr kinase under certain conditions.

Clustering of Phosphorylation Sites in the N-Terminal Region

Notably, the most phosphorylated Ser/Thr residues identified in this study on pollen occur in the poorly conserved N-terminal region. Many of the other plant sPPase phosphorylation sites are clustered in the 36- to 57-amino acid N-terminal region of low homology. A feature of sPPases from eukaryotes is that they have variable N- or C-terminal extensions, which are absent from well-characterized prokaryotic sPPases (Supplemental Fig. S5); however, their function is unknown. As the *E. coli* sPPase is fully active and these N- and C-terminal extensions are absent, it is assumed that they are nonessential for catalytic activity. However, clearly, phosphorylation in these regions can affect sPPase activity. For plant sPPases, these N-terminal extensions have been modeled and postulated to be involved in the regulation of enzyme activity (Rosales-León et al., 2012). Although a crystal structure for a Family I sPPase was solved recently for plants (Grzechowiak et al., 2013), the structure does not include an N-terminal extension. Nevertheless, our results and a survey of public phosphoproteomic databases provide many examples in which eukaryotic sPPase have been observed with phosphorylation sites clustered in their variable N-terminal regions. From primary sequence comparisons of p26a/b with other sPPases in combination with our data, we tentatively suggest that phosphomodification of the N and C termini may affect eukaryotic PPase activity. While it is

sPPases (Rudd et al., 1996; de Graaf et al., 2006). Here, we have mapped several phosphorylation sites on these proteins using both endogenous pollen kinases and recombinant CPKs and identified multiple (and different) phosphorylation sites on p26a and p26b in their N termini. We queried the P³DB plant phosphorylation database (www.p3db.org) for other phosphorylated sPPases using BLAST analyses with p26a/b sequences. This identified phosphorylated sites on several eukaryotic sPPases. The plant sPPases, including Arabidopsis, maize (*Zea mays*), rice (*Oryza sativa*), and grape (*Vitis vinifera*), had the majority of phosphorylation sites located within their N termini (Supplemental Fig. S5). Although there are now several large-scale phosphoproteomic analyses, to our knowledge, no reports in the literature have discussed the direct mapping of phosphorylation sites on sPPases from any organism. Many of the phosphorylation sites on sPPases are clustered within the variable N- and C-terminal extensions that appear to be a feature of eukaryotic sPPases rather than in the conserved catalytic region; we discuss these below. As no phosphomodifications were

not yet clear how these regions might regulate enzyme activity, evidence provided here gives an example in which phosphomimic changes in N-terminal regions can make sPPases more sensitive to inhibitory conditions. It is also possible that these phosphomodifications could have synergistic impacts in vivo, for example, by promoting or inhibiting protein-protein interactions. This merits investigation in the future.

CPKs Are Involved in the Phosphorylation of Plant sPPases

Our identification of CPKs as capable of phosphorylating these sPPases is a milestone, as, to date, few kinases responsible for phosphorylating eukaryotic sPPases have been identified. Not only did we identify CPK-dependent phosphorylation sites on p26a/b, but we also identified in the phosphoproteomic databases several other plant sPPases that were phosphorylated at sites in common with p26a/b, including several consensus CPK sites (basic-xxS/T and S-x-basic; Roberts and Harmon, 1992; Neumann et al., 1996; Harper and Harmon, 2005; Curran et al., 2011). For example, the region $RILS_{27}S_{28}LS_{30}RR$ is phosphorylated in p26a and appears to be conserved in several plant sPPases. Within this region is an RxxSxx substrate motif for CPKs and Ca^{2+}/calmodulin-dependent kinase (Mayank et al., 2012). While these data demonstrate that sPPases can be phosphorylated by CPKs, it is also possible that in planta regulation of sPPases could be mediated by other kinases that phosphorylate the same or different sites.

What Is the Biological Significance of sPPase Phosphorylation?

Although PPi activity in eukaryotic cells is critically important (Chen et al., 1990; Sonnewald, 1992; de Graaf et al., 2006; George et al., 2010), to date, very few studies of the mechanisms underlying the regulation of PPi homeostasis (in eukaryotes in particular) have been reported. Our findings substantially improve the knowledge of how sPPases can be posttranslationally modified to affect their activity. With the exception of a single article, reporting in vitro phosphorylation of rat liver sPPase by cAMP-dependent protein kinase (increasing its activity; Vener et al., 1990), to our knowledge, there have been no other reports of phosphorylation affecting Family I sPPase activity. Our findings here identify and suggest that multiple phosphorylation sites play a role in modulating the sensitivity of these sPPases to inhibition by several physiologically relevant cellular conditions. We showed that the phosphomimic forms of p26a/b are more responsive to inhibition by Ca^{2+}, and even more so to Ca^{2+} combined with H_2O_2, and that PPase activity can be modulated by lowered $[pH]_{cyt}$. Thus, these conditions allowed us to establish which

phosphorylation sites are important for modulating their PPase activity.

As both Ca^{2+} and ROS are stimulated very rapidly by SI, this suggests that SI not only stimulates the phosphorylation of p26 but that cellular conditions stimulated by SI contribute to the further reduction of PPase activity (and have a greater effect on the activity of the phosphorylated forms). Moreover, our data suggest that the slightly later pH drop stimulated by SI can further reduce the p26 sPPase activities. Together, our data indicate that all of these SI-triggered intracellular events are likely to contribute to the reduction in PPase activity. Thus, our findings have high biological relevance in the SI system. Whether the PPase phosphorylation is absolutely required for SI is difficult to assess; however, it clearly occurs, and this can alter activity under certain conditions. It would be of interest to examine whether other plant sPPases might be regulated in this manner. This is something that should be explored in the future.

As ROS play a pivotal role in many stress pathways, including apoptosis and PCD (Gadjev et al., 2008; Van Breusegem et al., 2008; Circu and Aw, 2010), this provides a significant advance in our understanding of the mechanisms regulating this important class of enzymes. Not only are our observations placed in a physiologically relevant context for SI in pollen, but it also provides, to our knowledge, the first demonstration of pH affecting the sensitivity of sPPase activity in combination with phosphorylation. The role of $[pH]_{cyt}$ in modulating physiological processes in eukaryotic cells has been largely ignored until recently, when two

Table I. *Primers used for CPK cloning*

Primer	Sequence 5′→3′
CPK-F	GAGGATGTTAGGAGGGAGGTTG AGATTATG
CPK-R	TCAGTCTCTGCCCAAAATGGCGG AACACCAC
3′RACE 17AP	GACTCGAGTCGACATCGATTTTTTT TTTTTTTTTTT
3′RACE UAP	GACTCGAGTCGACATCGA
5′RACE AAP	GGCCACGCGTCGACTAGTACGGG55 GGG55GGG55G
5′RACE UAP	GGCCACGCGTCGACTAGTAC
CPK17/34-3′RACE1	GCAAATTGTTCATACTTGTCATTCAAT
CPK14-3′RACE1	GTTGTTCAGATGTGTCACAAGCAC
CPK6/26-3′RACE1	GTGAACAAGGATGATGATTTTTCTCTC
CPK17/34-3′RACE2	TTTCAGGGATATTGTGGGTAGTGC
CPK14-3′RACE2	GTTTACTGAGATAGTTGGAAGCCC
CPK6/26-3′RACE2	GCTCCCGAGGTACTTTGCAAAC
CPK17/34-5′RACE1	CAATTTGCACTATCGTTCTTAATAAAG
CPK14-5′RACE1	CTTCGACAATTGTACGAGTAACTAC
CPK6/26-5′RACE1	CTCATAAGCACCCTTGATCGTC
CPK17/34-5′RACE2	CATAACCAAATGCACAGATTGCTTATC
CPK14-5′RACE2	CATTACAAGATGTACAGCATTATCG
CPK6/26-5′RACE2	CTCCATGACAATATGAACATACAACG
CPK17/34-5′RACE3	CCACCATGGGTAATTGTTGCCC
CPK14-5′RACE3	GAATAATAATATAGGAAGCTTTGATCC
CPK6/26-5′RACE3	CTATCGAACAATTCACCTCCAGAG

studies showed that shifting $[pH]_{cyt}$ is pivotal in triggering PCD (Fendrych et al., 2014; Wilkins et al., 2015). It was suggested that the gateway to PCD could be cytosolic acidification, when the drop in $[pH]_{cyt}$ passes a threshold and this activates caspase-3-like/DEVDase (which is normally inactive at pH 7). Our study here suggests that the phosphorylation of sPPases also can be modulated by lowered $[pH]_{cyt}$ and identifies several amino acids as being involved in the modulation of PPase activity by amplifying pH sensitivity.

Many cellular processes are regulated by reversible protein phosphorylation, and identifying the targets, sites, and protein kinases involved is crucial to understand how these important posttranslational modifications affect biological function (Humphrey et al., 2015). Although many target kinases are known to be phosphorylated, few nonsignaling proteins have been highlighted (Mayank et al., 2012). The finding that pollen sPPases are targets of phosphorylation and that this can affect activity suggests that this might be an important way to simultaneously inhibit a large number of metabolic processes that require sPPase activity as part of a thermodynamically coupled reaction. As PPases can regulate many pathways, this suggests that they might act as a master regulator. Future studies should investigate these aspects further, testing the possibility that sPPases could be a regulatory hub where their phosphoinhibition might trigger global changes in cellular metabolism in other cell types and responses other than pollen SI.

MATERIALS AND METHODS

His Tag Affinity Purification of Recombinant p26 Proteins

C-terminal His-tagged recombinant p26 proteins (de Graaf et al., 2006) were expressed from pET21b (Novagen) in Luria-Bertani medium (100 μg mL^{-1} ampicillin) supplemented with 2 mM MgCl$_2$ to allow optimal activity after purification. Protein expression was induced in *Escherichia coli* BL21 using 1 mM isopropyl-β-D-1-thiogalactopyranoside at 22°C. Proteins were purified using a nickel-nitrilotriacetic acid (Ni-NTA) agarose FPLC column or Ni-NTA spin columns (Qiagen).

Cloning of *PrCPKs*

cDNA was synthesized using the Invitrogen SuperScript II Reverse Transcriptase kit using total RNA extracted from *Papaver rhoeas* pollen (RNeasy Plant Mini Kit; Qiagen). Degenerate primers (CPK-F and CPK-R) based on Arabidopsis (*Arabidopsis thaliana*) CPKs were then used to obtain partial pollen-expressed *P. rhoeas* CPK cDNAs (Table I). Full-length cDNAs of *PrCPK14*, *PrCPK6/26*, and *PrCPK17/34* were then obtained using a combination of 3' and 5' RACE PCR. 3' RACE amplification was carried out on *P. rhoeas* pollen cDNA using a 3' RACE primer (3'RACE 17AP) and 5' gene-specific primers (3'RACE1). The product was PCR purified and reamplified with a 3' RACE primer (3'RACE UAP) and nested gene-specific 5' primers (3'RACE2). For 5' RACE, cDNA was synthesized using a primer specific to the 3' end of the gene of interest (5'RACE1) instead of the oligo(dT) primer. cDNA was cleaned up using the QIAquick PCR Purification Kit (Qiagen). A tailing reaction was then performed to add a poly(C) tail at the 5' end. PCR amplification was then carried out with a 5' RACE abridged primer (5'RACE AAP) and a second gene-specific 3' primer (5'RACE2). This amplification product was PCR purified and then reamplified with a 5' RACE unabridged primer (5'RACE UAP) and a third nested gene-specific 3' primer (5'RACE3).

Phylogenetic analysis of Arabidopsis and *P. rhoeas* CPKs was performed using PhyML (www.phylogeny.lirmm.fr).

His Tag Affinity Purification of Recombinant CPK Proteins

His-tagged recombinant CPKs were made using pET21b (Novagen). Protein expression was induced in *E. coli* BL21 Rosetta (Novagen) using 1 mM isopropyl-β-D-1-thiogalactopyranoside at 22°C for 16 h. Cell pellets were resuspended and lysed in 50 mM Tris-HCl, pH 8, 0.1 M NaCl, 5 mM EDTA, 1 mM EGTA, 0.5 mM 4-(2-Aminoethyl)benzenesulfonylfluoride, HCl (Calbiochem), cOmplete EDTA-free protease inhibitor cocktail (Roche Diagnostics), and 0.5 mg mL^{-1} lysozyme. Cleared lysate was dialyzed against 20 mM Tris-HCl (pH 8) and 0.1 M NaCl to remove trace calcium. CPKs were isolated using 1 mL of Ni-NTA agarose resin (Qiagen) at 4°C and eluted with 50 mM Tris-HCl, pH 8, 0.1 M NaCl, and 250 mM imidazole. Pooled eluate fractions were precipitated using 0.5 M ammonium sulfate and cleared supernatant applied to a HiTrap Phenyl HP column (GE Healthcare), washed with 20 mM Tris-HCl, pH 8 and 0.5 M ammonium sulfate, and eluted with a reverse gradient to 20 mM Tris-HCl, pH 8 (0.5 mL min^{-1}). Fractions were concentrated using a Sartorius Vivaspin 500 (10,000 molecular weight cutoff) and applied to Superdex 200 26/60 (GE Healthcare) equilibrated with 20 mM Tris-HCl, pH 8, and 0.1 M NaCl.

Site-Directed Mutagenesis

Triple, quintuplet, and septuplet phosphomimic and phosphonull phosphorylation site substitution mutants of p26a (3E/3A, 5E/5A, and 7E/7A, respectively) and p26b (3'E/3'A, 5'E/5'A, and 7'E/7'A, respectively) were constructed using the Quikchange II Site Directed Mutagenesis Kit (Agilent Technologies). Mutagenic primers were designed according to the manufacturer's instructions using GenBank sequences for p26.1a (AM162550.1) and p26.1b (AM162551.1). The mutants, together with their amino acid substitutions, are listed in Supplemental Table 3, A and B.

PPase Assays

Recombinant His-tagged p26 proteins or their substitution mutant versions were diluted to 10 μM in 50 mM HEPES-KOH, pH 8, 50 μM EGTA, and 2 mM MgCl$_2$. Aliquots of 250 ng were assayed for free phosphate using a discontinuous PPase assay, adapted from the method of Fiske and Subbarow (1925), using 2 mM sodium pyrophosphate (or other substrate as appropriate). The assay buffer was supplemented with 2 mM MgCl$_2$ (or other metal salts/inhibitors as appropriate) or 0.1 mM CaCl$_2$ and/or 10 mM H$_2$O$_2$. Assays requiring a pH range used 50 mM propionic acid, pH 5 to 7. To measure the effect of divalent cations other than Mg^{2+}, His-tagged p26 proteins were incubated with the appropriate metal salts for 2 h prior to assay.

The continuous method for monitoring orthophosphate was adapted from Baykov and Avaeva (1981). An aliquot of p26 was injected into a continuous flow system containing a 15-mL mixing chamber equilibrated with 40 mM HEPES, pH 7.2, 50 μM EGTA, 5 mM MgCl$_2$, and 0 to 500 μM sodium pyrophosphate. PPase activity was measured continuously at pH 7.2 and 30°C by the addition of 0.0096% (w/v) Methyl Green in 0.18% (v/v) Triton X-305 and 5.7% (w/v) ammonium molybdate in 18.3% (v/v) H$_2$SO$_4$ and then monitored at 650 nm using a UA-6 ISCO flow-through detector (Ilias, 2004). Duplicate data were prepared from independent protein preparations and solved for K_m and k_{cat} using the curve-fit program SigmaPlot (Systat Software).

Kinase Assays for Mapping Phosphorylation Sites

In vitro kinase assays using pollen protein were performed according to Rudd et al. (1996). Briefly, pollen was homogenized on ice for 15 min in 50 mM Tris-HCl, pH 7.5, and 0.1% Triton X-100 containing cOmplete EDTA-free protease inhibitor cocktail (Roche Diagnostics), cell debris was removed by centrifugation, and supernatants were stored at −20°C until use. Recombinant His-tagged p26 was incubated with 100 μg of crude pollen extract in 50 mM Tris-HCl, pH 7.5, 1 mM ATP, 1 mM MgCl$_2$, and 0.25 mM calyculin A for 15 min at 30°C. The p26 was isolated using Ni-NTA spin columns (Qiagen), digested with trypsin, and analyzed using LC-MS/MS (see below). Recombinant His-tagged p26 proteins also were incubated with recombinant His-tagged CPKs in kinase buffer (50 mM Tris-HCl, pH 7.5, 1 mM ATP, 10 mM MgCl$_2$, and 0.1 mM CaCl$_2$) for 30 min. Aliquots were digested with either trypsin or endoproteinase Glu-C and analyzed using LC-MS/MS.

In Vitro Kinase Activity Assays

The incorporation of ^{32}P into recombinant His-tagged purified p26 proteins (de Graaf et al., 2006) in the presence/absence of 50 ng of recombinant CPKs (Harper et al., 1994) was determined after a 10-min reaction at 30°C. One microliter of 4,000 Ci mmol^{-1} [γ-^{32}P]ATP was added to a 50-μL reaction mix on ice (50 mM HEPES-KOH, pH 7.7, 5 mM MgCl$_2$, 0.5 mM dithiothreitol, 300 μM ATP, and 1.1 mM CaCl$_2$) and transferred to 30°C after 1 min. The reaction was stopped by adding protein-loading dye. The phosphorylation of p26a/b was analyzed using SDS-PAGE followed by autoradiography and scanning for relative labeling or scintillation counting (Tri-Carb 2810 TR Liquid Scintillation Analyzer; PerkinElmer).

For the kinetic kinase assays, purified recombinant His-tagged CPKs were assayed (Curran et al., 2011) over a time course using standard filter-based kinase assays to measure the total incorporation of ^{32}P into p26. Briefly, 25-μL kinase reactions contained 1 ng μL^{-1} CPK His-tagged fusion protein in 20 mM Tris-HCl, pH 7.5, 10 mM MgCl$_2$, 1 mM EGTA, 1.1 mM CaCl$_2$, and 0.1 mg mL^{-1} bovine serum albumin with varied syntide-2 (Sigma-Aldrich) substrate concentrations. Reactions were initiated by the addition of 50 μM ATP spiked with 0.375 μCi of [γ-^{32}P]ATP (3,000 Ci mmol^{-1}; PerkinElmer) and incubated at room temperature for 10 min. Total ^{32}P counts incorporated into the substrate were determined by Cerenkov counting on a Tri-Carb 2810 TR Liquid Scintillation Analyzer (PerkinElmer). Activities were calculated as nmol phosphate incorporated min^{-1} mg^{-1} CPK moiety. K_m and k_{cat} were determined by curve fitting using SigmaPlot 11.0. K_m and k_{cat} were determined as means from two independent data curves for two independent preparations.

Digestion and Enrichment of Proteins for Mass Spectrometry

Proteins were digested using either Trypsin Gold (Promega) or Endoproteinase GluC (New England Biolabs) according to the manufacturer's instructions. Briefly, 10 mM dithiothreitol was added to the protein, which was incubated in 100 mM ammonium bicarbonate (pH 8) at 56°C for 30 min. Samples were cooled to room temperature, and Cys residues were alkylated by the addition of 50 mM iodoacetamide (50 μL) and incubated in the dark for 30 min. Digested samples were enriched for phosphopeptides using the Titansphere Phos-TiO Kit (GL Sciences). Samples were dried and resuspended in 50 μL of buffer B (25% lactic acid) plus 75% buffer A (2% trifluoroacetic acid in 80% acetonitrile) and loaded onto prepared Spin Tips, centrifuged, and rinsed in buffers B and A. Phosphopeptides were eluted in 5% ammonium hydroxide, dried, and resuspended in 2% trifluoroacetic acid for desalting. Samples were desalted using ZipTip$_{C18}$ (Merck Millipore) according to the manufacturer's instructions, and peptides were eluted with 10 μL of 50% acetonitrile/0.1% trifluoroacetic acid, dried, and resuspended in 0.1% formic acid.

LC-MS/MS

Phosphorylated peptides enriched from the tryptic digest were concentrated and separated using an UltiMate 3000 nano-HPLC series (Dionex). Samples were trapped on a μPrecolumn Cartridge (Acclaim PepMap 100 C18, 5 μm, 100 Å, 300 μm i.d. × 5 mm; Dionex) and separated in Nano Series Standard Columns (75 μm i.d. × 15 cm, packed with C18 PepMap100, 3 μm, 100 Å; Dionex) using a 3.2% to 44% solvent B (0.1% formic acid in acetonitrile) gradient for 30 min. Peptides were eluted directly (~350 nL min^{-1}) via a TriVersaNanoMate nanospray source (Advion Biosciences) into the LTQ Velos with Orbitrap ETD mass spectrometer (Thermo Fisher Scientific). Data-dependent scanning acquisition was controlled by Xcalibur 2.1 software (Thermo Fisher Scientific).

Phosphopeptides were analyzed by collision-induced dissociation (CID) neutral loss-triggered ETD. A full Fourier transform-mass spectrometry scan (m/z 380–1,600) and subsequent CID tandem mass spectrometry (MS/MS) scans of the 20 most abundant ions were performed. Survey scans were acquired in the Orbitrap with a resolution of 30,000 at m/z 400 and automatic gain control (AGC) 1 × 10^6. Precursor ions were isolated and subjected to CID in the linear ion trap with AGC 1 × 10^5. Collision activation for the experiment was performed in the linear trap using helium gas at normalized collision energy to precursor m/z of 35% and activation Q of 0.25. If neutral loss of 98 D from the precursor ion was observed in the CID MS/MS spectrum, ETD from the same precursor ion was triggered in the linear ion trap. Isolation width was 2 m/z, AGC target 1 × 10^5, and maximum inject time 50 ms. ETD was performed with fluoranthene ions, and the AGC target for fluoranthene ions was 1 × 10^6 (maximum fill time, 50 ms). Precursor ions were activated for 130 ms, and supplemental activation was performed with normalized collision energy of 25%.

CID MS/MS and ETD MS/MS data were searched against National Center for Biotechnology Information nonredundant Green Plant database using the SEQUEST algorithm (Thermo Scientific). Modifications searched for were deamidation (N and Q), oxidation (M), and phosphorylation on Ser, Thr, and Tyr. Two missed cleavages were allowed. The precursor mass tolerance was 5 ppm, and the MS/MS mass tolerance was 0.8 D with false discovery rate of 1%. Phosphorylation sites identified in sPPases were collated from BLAST search analyses, using the p26a and p26b sequences, in publicly available databases: www.p3db.org, www.phosphat.uni-hohenheim.de, www.phosida.com, www.phosphosite.org, www.UniProtKB.org, www.phosphgrid.org, and www.phosphopep.org. Sequence alignments were performed using Clustal Omega (www.ebi.ac.uk/Tools/msa/clustalo/).

Accession Numbers

P. rhoeas CPK gene sequences are available at the European Nucleotide Archive at http://www.ebi.ac.uk/ena/data/view/ with accession numbers LT605077 (*CPK14*), LT605078 (*CPK17/34*), and LT605079 (*CPK6/26*).

Supplemental Data

The following supplemental materials are available.

Supplemental Figure S1. Amino acids phosphorylated by endogenous pollen kinases in p26 sPPases.

Supplemental Figure S2. General properties of p26a/b sPPases.

Supplemental Figure S3. Sequence homology between *P. rhoeas* and Arabidopsis CPKs.

Supplemental Figure S4. Autophosphorylation sites mapped in CPKs.

Supplemental Figure S5. Phosphorylation sites identified on sPPases.

Supplemental Table S1. Substrate specificity of p26 sPPases.

Supplemental Table S2. Locations of phosphorylated rtitesidues identified in recombinant p26a and p26b.

Supplemental Table S3. Kinetic assessment of recombinant CPK activity using syntide-2 as substrate and of p26 proteins as substrates for CPKs in vitro.

Supplemental Table S4. Phosphomimic/phosphonull mutants of p26a and p26b and kinetic parameters of pyrophosphate hydrolysis by p26a and p26b and their phosphomimic/phosphonull mutants.

Supplemental Table S5. Mapping of phosphopeptides in recombinant PrCPKs autophosphorylated during in vitro phosphorylation assays using LC-MS/MS.

Supplemental Data S1. Supplemental Data Appendices 1–13.

LITERATURE CITED

Baykov AA, Avaeva SM (1981) A simple and sensitive apparatus for continuous monitoring of orthophosphate in the presence of acid-labile compounds. Anal Biochem **116:** 1–4

Bosch M, Franklin-Tong VE (2007) Temporal and spatial activation of caspase-like enzymes induced by self-incompatibility in Papaver pollen. Proc Natl Acad Sci USA **104:** 18327–18332

Buchanan B, Gruissem W, Jones R, editors (2002) Biochemistry and Molecular Biology of Plants. Wiley-Blackwell, New Jersey

Chen J, Brevet A, Fromant M, Lévêque F, Schmitter JM, Blanquet S, Plateau P (1990) Pyrophosphatase is essential for growth of *Escherichia coli*. J Bacteriol **172:** 5686–5689

Circu ML, Aw TY (2010) Reactive oxygen species, cellular redox systems, and apoptosis. Free Radic Biol Med **48:** 749–762

Cooperman BS, Baykov AA, Lahti R (1992) Evolutionary conservation of the active site of soluble inorganic pyrophosphatase. Trends Biochem Sci **17:** 262–266

Curran A, Chang IF, Chang CL, Garg S, Miguel RM, Barron YD, Li Y, Romanowsky S, Cushman JC, Gribskov M, et al (2011) Calcium-dependent protein kinases from Arabidopsis show substrate specificity differences in an analysis of 103 substrates. Front Plant Sci 2: 36

de Graaf BHJ, Rudd JJ, Wheeler MJ, Perry RM, Bell EM, Osman K, Franklin FCH, Franklin-Tong VE (2006) Self-incompatibility in *Papaver* targets soluble inorganic pyrophosphatases in pollen. Nature 444: 490–493

Fendrych M, Van Hautegem T, Van Durme M, Olvera-Carrillo Y, Huysmans M, Karimi M, Lippens S, Guérin CJ, Krebs M, Schumacher K, et al (2014) Programmed cell death controlled by ANAC033/SOMBRERO determines root cap organ size in Arabidopsis. Curr Biol 24: 931–940

Fiske CH, Subbarow Y (1925) The colorimetric determination of phosphorous. J Biol Chem 66: 375–400

Foote HCC, Ride JP, Franklin-Tong VE, Walker EA, Lawrence MJ, Franklin FCH (1994) Cloning and expression of a distinctive class of self-incompatibility (S) gene from *Papaver rhoeas* L. Proc Natl Acad Sci USA 91: 2265–2269

Franklin-Tong VE, Hackett G, Hepler PK (1997) Ratio-imaging of $[Ca^{2+}]_i$ in the self-incompatibility response in pollen tubes of *Papaver rhoeas*. Plant J 12: 1375–1386

Gadjev I, Stone JM, Gechev TS (2008) Programmed cell death in plants: new insights into redox regulation and the role of hydrogen peroxide. Int Rev Cell Mol Biol 270: 87–144

George GM, van der Merwe MJ, Nunes-Nesi A, Bauer R, Fernie AR, Kossmann J, Lloyd JR (2010) Virus-induced gene silencing of plastidial soluble inorganic pyrophosphatase impairs essential leaf anabolic pathways and reduces drought stress tolerance in *Nicotiana benthamiana*. Plant Physiol 154: 55–66

Grzechowiak M, Sikorski M, Jaskolski M (2013) Inorganic pyrophosphatase (PPase) from a higher plant. BioTechnologia 94: 35–37

Harper JF, Breton G, Harmon A (2004) Decoding Ca^{2+} signals through plant protein kinases. Annu Rev Plant Biol 55: 263–288

Harper JF, Harmon A (2005) Plants, symbiosis and parasites: a calcium signalling connection. Nat Rev Mol Cell Biol 6: 555–566

Harper JF, Huang JF, Lloyd SJ (1994) Genetic identification of an auto-inhibitor in CDPK, a protein kinase with a calmodulin-like domain. Biochemistry 33: 7267–7277

Humphrey SJ, James DE, Mann M (2015) Protein phosphorylation: a major switch mechanism for metabolic regulation. Trends Endocrinol Metab 26: 676–687

Ilias M (2004) Family II soluble inorganic pyrophosphatases from *Streptococcus gordonii* and *Vibrio cholerae*. PhD thesis. University of Birmingham, Birmingham, UK

Kukko-Kalske E, Lintunen M, Inen MK, Lahti R, Heinonen J (1989) Intracellular PPi concentration is not directly dependent on amount of inorganic pyrophosphatase in *Escherichia coli* K-12 cells. J Bacteriol 171: 4498–4500

Mayank P, Grossman J, Wuest S, Boisson-Dernier A, Roschitzki B, Nanni P, Nühse T, Grossniklaus U (2012) Characterization of the phosphoproteome of mature Arabidopsis pollen. Plant J 72: 89–101

Myers C, Romanowsky SM, Barron YD, Garg S, Azuse CL, Curran A, Davis RM, Hatton J, Harmon AC, Harper JF (2009) Calcium-dependent protein kinases regulate polarized tip growth in pollen tubes. Plant J 59: 528–539

Neumann GM, Thomas I, Polya GM (1996) Identification of the site on potato carboxypeptidase inhibitor that is phosphorylated by plant calcium-dependent protein kinase. Plant Sci 114: 45–51

Ogasawara N (2000) Systematic function analysis of *Bacillus subtilis* genes. Res Microbiol 151: 129–134

Oh MH, Wu X, Kim HS, Harper JF, Zielinski RE, Clouse SD, Huber SC (2012) CDPKs are dual-specificity protein kinases and tyrosine autophosphorylation attenuates kinase activity. FEBS Lett 586: 4070–4075

Pérez-Castiñeira JR, López-Marqués RL, Villalba JM, Losada M, Serrano A (2002) Functional complementation of yeast cytosolic pyrophosphatase by bacterial and plant H^+-translocating pyrophosphatases. Proc Natl Acad Sci USA 99: 15914–15919

Rajagopal L, Clancy A, Rubens CE (2003) A eukaryotic type serine/threonine kinase and phosphatase in *Streptococcus agalactiae* reversibly phosphorylate an inorganic pyrophosphatase and affect growth, cell segregation, and virulence. J Biol Chem 278: 14429–14441

Roberts DM, Harmon AC (1992) Calcium-modulated proteins: targets of intracellular calcium signals in higher plants. Annu Rev Plant Physiol Plant Mol Biol 43: 375–414

Rosales-León L, Hernández-Domínguez EE, Gaytán-Mondragón S, Rodríguez-Sotres R (2012) Metal binding sites in plant soluble inorganic pyrophosphatases: an example of the use of ROSETTA design and hidden Markov models to guide the homology modeling of proteins. J Mex Chem Soc 56: 23–31

Rudd JJ, Franklin F, Lord JM, Franklin-Tong VE (1996) Increased phosphorylation of a 26-kD pollen protein is induced by the self-incompatibility response in *Papaver rhoeas*. Plant Cell 8: 713–724

Serrano-Bueno G, Hernández A, López-Lluch G, Pérez-Castiñeira JR, Navas P, Serrano A (2013) Inorganic pyrophosphatase defects lead to cell cycle arrest and autophagic cell death through NAD^+ depletion in fermenting yeast. J Biol Chem 288: 13082–13092

Sonnewald U (1992) Expression of *E. coli* inorganic pyrophosphatase in transgenic plants alters photoassimilate partitioning. Plant J 2: 571–581

Sugiyama N, Nakagami H, Mochida K, Daudi A, Tomita M, Shirasu K, Ishihama Y (2008) Large-scale phosphorylation mapping reveals the extent of tyrosine phosphorylation in Arabidopsis. Mol Syst Biol 4: 193

Van Breusegem F, Bailey-Serres J, Mittler R (2008) Unraveling the tapestry of networks involving reactive oxygen species in plants. Plant Physiol 147: 978–984

Vener AV, Smirnova IN, Baykov AA (1990) Phosphorylation of rat liver inorganic pyrophosphatase by ATP in the absence and in the presence of protein kinase. FEBS Lett 264: 40–42

Wheeler MJ, de Graaf BHJ, Hadjiosif N, Perry RM, Poulter NS, Osman K, Vatovec S, Harper A, Franklin FCH, Franklin-Tong VE (2009) Identification of the pollen self-incompatibility determinant in *Papaver rhoeas*. Nature 459: 992–995

Wilkins KA, Bancroft J, Bosch M, Ings J, Smirnoff N, Franklin-Tong VE (2011) Reactive oxygen species and nitric oxide mediate actin reorganization and programmed cell death in the self-incompatibility response of *Papaver*. Plant Physiol 156: 404–416

Wilkins KA, Bosch M, Haque T, Teng N, Poulter NS, Franklin-Tong VE (2015) Self-incompatibility-induced programmed cell death in field poppy pollen involves dramatic acidification of the incompatible pollen tube cytosol. Plant Physiol 167: 766–779

Wilkins KA, Poulter NS, Franklin-Tong VE (2014) Taking one for the team: self-recognition and cell suicide in pollen. J Exp Bot 65: 1331–1342

Wu J, Wang S, Gu Y, Zhang S, Publicover SJ, Franklin-Tong VE (2011) Self-incompatibility in *Papaver rhoeas* activates nonspecific cation conductance permeable to Ca^{2+} and K^+. Plant Physiol 155: 963–973

Zulawski M, Schulze G, Braginets R, Hartmann S, Schulze WX (2014) The Arabidopsis kinome: phylogeny and evolutionary insights into functional diversification. BMC Genomics 15: 548